Structure and Reactivity in Langmuir Films of Amphiphilic Alkyl and Thio-alkyl Esters of α-Amino Acids at the Air/Water Interface

Ran Eliash,[†] Isabelle Weissbuch,[†] Markus J. Weygand,[‡] Kristian Kjaer,[‡] Leslie Leiserowitz,[†] and Meir Lahav*[,†]

Department of Materials and Interfaces, The Weizmann Institute of Science, 76100 Rehovot, Israel, and Materials Research Department, Risø National Laboratory, 4000 Roskilde, Denmark

Received: February 11, 2004; In Final Form: March 24, 2004

The structure and reactivity of alkyl esters of several α-amino acids self-assembled at the air/water interface have been investigated as part of our studies on mechanisms that are possibly relevant for the generation of homochiral prebiotic peptides. Grazing incidence X-ray diffraction (GIXD) studies of monolayers of racemic and enantiopure alkyl esters and thio-esters of alanine on the water surface demonstrated that these racemates self-assemble in the form of mixed solid solutions, because of disorder of the headgroups of the two enantiomers (enantiomeric disorder) within the two-dimensional (2D) crystallites. Matrix-assisted laser-desorption ionization time-of-flight Mass Spectrum (MALDI−TOF MS) analysis of the products collected from the air/water interface indicated the formation of low-molecular-weight oligopeptides (primarily dimers) and, in the case of some of the thioesters, small quantities of trimers and tetramers. Mass spectrometric studies on the diastereoisomeric distribution of the oligopeptides, starting from deuterium enantio-labeled monomers, demonstrated binomial statistics, such as that in reactions occurring in an isotropic environment. The alkyl esters of phenylalanine and tyrosine did not form 2D crystallites at the air/water interface, and, upon polycondensation, they yielded only dipeptides. The enantiomeric disorder within the 2D crystallites of the monomers of the alkyl esters and thioesters of racemic serine was absent. Polycondensation of these esters, however, yielded only dipeptides and tripeptides and they were not investigated further. In contrast to previous reports, the present studies demonstrate that this reaction does not proceed beyond the dipeptide stage and, therefore, cannot be regarded as a plausible system for the generation of prebiotic peptides.

1. Introduction

The emergence of peptides of single handedness and homochiral sequence (isotactic) from racemic α-amino acids in abiotic times is one of the most interesting riddles in the field of the origin of life.[1,2] Recently, we have presented an experimental model for the formation of enantiopure isotactic oligopeptides from nonracemic mixtures of activated amino acids bearing long hydrocarbon chains at their α-carbon.[3−7] This methodology is comprised of two sequential steps: self-assembly of the amphiphilic amino acids into two-dimensional (2D) crystallites on the water surface or in a phospholipid environment, followed by a lattice-controlled polymerization to form the corresponding oligopeptides. In these systems, however, the oligopeptides products bear long hydrocarbon chains.

Previously, it has been reported that Langmuir and Langmuir−Blodgett films of long-chain alkyl esters of amino acids both in their enantiopure and racemic forms undergo polycondensation by a simple "unzipping" mechanism,[8−11] as illustrated in Scheme 1. Based on kinetic studies, it was proposed that, in these systems, the reaction rate was enhanced by the lateral molecular order within the film, yielding peptides in the form of α-helixes or β-sheets.[12,13] The formation of secondary structure implies that these peptides contained at least eight repeating units.[14,15] Based on these reports, we considered that such monomers can provide ideal intermediates for the generation of natural oligopeptides by a process of their unzipping from membranes or from vesicles. The reported formation of the peptide bond was demonstrated either by infrared (IR) spectroscopy,[9−13] ninhydrin analysis,[8] or surface viscosity.[9] Although these analytical methods reveal the formation of a peptide bond, they do not provide information regarding the molecular weight and enantiomeric composition of the peptides. To probe the potential future application of this reaction as a useful reaction model system in prebiotic chemistry, we reinvestigated the reactivity of several molecules previously reported,[9−13] as well as some additional alkyl esters and thioesters of α-amino acids. We applied the grazing incidence X-ray diffraction (GIXD) technique to determine the packing arrangement of the monomer molecules within the 2D self-assemblies and matrix-assisted laser-desorption ionization time-of-flight mass spectrometry (MALDI−TOF MS) for the determination of the molecular weight distribution of the peptides. For some of the systems, the diastereoisomeric composition of the oligopeptides was deduced by polymerizing monomers enantioselectively labeled with deuterium.

2. Experimental Section

2.1. Materials. Materials that were used in this study include protected amino acids (BACHEM AG and NovaBiochem), L-alanine(d_4) (MSD ISOTOPES), all solvents and reagents (BDH, Fluka, Aldrich, Sigma and Merck).

2.1.1. D-, L-, and DL-Alanine Octadecyl Ester (Ala-C_{18}). The free amine was prepared according to Penney et al.[16] and was

* Author to whom correspondence should be addressed: Telephone: (972)-8-934-2111. Fax (972)-8-934-4138. E-mail: meir.lahav@weizmann.ac.il.
[†] Weizmann Institute of Science.
[‡] Risø National Laboratory.

10.1021/jp049381j CCC: $27.50
Published on Web 05/07/2004

SCHEME 1: Proposed Mechanism of the "Unzipping" Polymerization, According to Fukuda et al.[11]

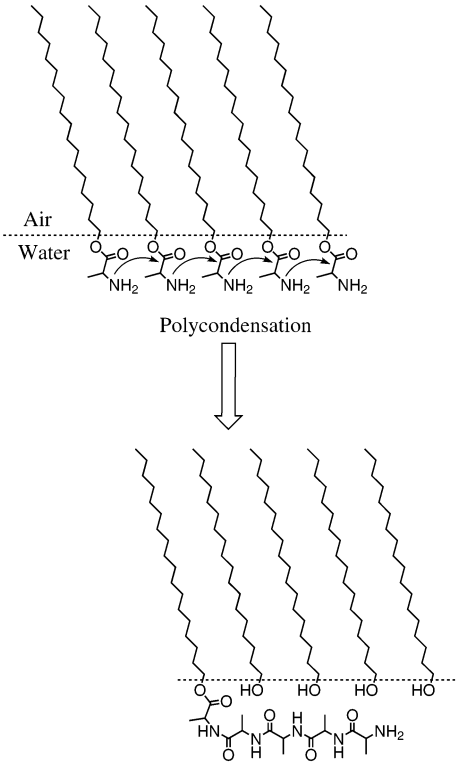

further purified by column chromatography (silica gel, ethyl acetate:*n*-hexane:acetone ratio of 5:4.5:0.5). ^{1}H NMR ($CDCl_3$ 250 MHz): $\delta = 0.88$(t, 3H; $C\underline{H}_3-[CH_2]_{15}-$), 1.30(br m, 33H; $CH_3-[C\underline{H}_2]_{15}-$; $-CHC\underline{H}_3NH_2$), 1.64(m, 2H; $-C\underline{H}_2CH_2OOC-$), 3.54(q, 1H; $-C\underline{H}CH_3NH_2$), 4.11(m, 2H; $-CH_2C\underline{H}_2OOC-$); ESI-MS: *m*/*z*: 364.58 [M^+ + Na]. Silica gel TLC, *n*-hexane: acetone ratio of 1:1, $R_f = 0.75$.

2.1.2. L- and DL-Phenylalanine Octadecyl Ester (Phe-C_{18}). The free amine was prepared according to Penney et al.[16] and purified by column chromatography (silica gel, ethyl acetate: *n*-hexane ratio of 2:3). ESI-MS: *m*/*z*: 418.64 [M^+ + H], 440.62 [M^+ + Na]. Silica gel TLC, ethyl acetate:*n*-hexane ratio of 2:3, $R_f = 0.30$.

2.1.3. D- and L-Tyrosine Octadecyl Ester (Tyr-C_{18}). The HCl salt was prepared according to Penney et al.[16] The free amine was released from the hydrochloride salt by extraction with a triethylamine/water mixture and recrystallized from *n*-hexane. ^{1}H NMR (5% CD_3OD in $CDCl_3$, 250 MHz): $\delta = 0.88$(t, 3H; $C\underline{H}_3-[CH_2]_{15}-$), 1.25(br m, 30H; $CH_3-[C\underline{H}_2]_{15}-$), 1.60(m, 2H; $-C\underline{H}_2CH_2OOC-$), 2.8−3.1(br m, 2H; $-C\underline{H}_2PhOH$), 3.73-(double d, 1H; $-C\underline{H}NH_2COO-$), 4.09(t, 2H; $-CH_2C\underline{H}_2OOC-$), 7.15−7.35(br m; aromatic hydrogens); ESI-MS: *m*/*z*: 434.43-[M^+ + H], 456.40[M^+ + Na]. Silica gel TLC, ethyl acetate: *n*-hexane:acetone ratio of 5:4:0.5, $R_f = 0.50$.

2.1.4. L- and DL-Glutamic Dioctadecyl Ester [Glu-$(C_{18})_2$]. The methylsulfonate salt was prepared according to Penney et al.[16] and recrystallized from CH_2Cl_2. The free amine was released from the hydrochloride salt by extraction with a triethylamine/ water mixture and recrystallized from a *n*-hexane/CH_2Cl_2 mixture. ESI-MS: *m*/*z*: 652.96[M^+ + H], 674.92[M^+ + Na]. Silica gel TLC, ethyl acetate:*n*-hexane:acetone ratio of 2:7:1, $R_f = 0.6$.

2.1.5. Octadecanamide *N*-Ethanol (C_{18}-AE). *N*-Hydroxysuccinimide ester of stearic acid[17] (5.29 g, 13.86 mmol, 1 equiv) and 2-aminoethanol (2.70 g, 44.2 mmol, 3.2 equiv) were dissolved in 140 mL of dry CH_2Cl_2. Triethylamine (2.10 g, 20.80 mmol, 1.5 equiv) that was dissolved in 5 mL of CH_2Cl_2 was added to the solution, resulting in the precipitation of a white solid. The reaction was allowed to stir for 2.5 h and then 500 mL of diethyl ether and 100 mL of ethanol were added to form a clear solution. The organic solution was washed with 0.5 M HCl (50 mL, three times), water (50 mL, two times) and dried with magnesium sulfate, and the solvent was evaporated in a vacuum. The resulting crystalline material was recrystallized from CH_2Cl_2 to give 4.01 g (88% yield) of pure octadecanamide *N*-ethanthiol. ^{1}H NMR ($CDCl_3$ 250 MHz): $\delta = 0.88$(t, 3H; $C\underline{H}_3-[CH_2]_{14}-$), 1.25(br m, 28H; $CH_3-[C\underline{H}_2]_{14}-$), 1.64(m, 2H; $-C\underline{H}_2CH_2CONH-$), 2.21(t, 2H; $-CH_2C\underline{H}_2CONH-$), 2.67(q, 2H; $-CONHCH_2C\underline{H}_2SH$), 3.43(q, 2H; $-CONHC\underline{H}_2CH_2SH$), 5.86(br s, 1H; $-CON\underline{H}-$); ESI-MS: *m*/*z*: 328.30[M^+ + H], 350.27[M^+ + Na].

2.1.6. Octadecanamide *N*-Ethanthiol (C_{18}-ATE). Same procedure as above, except that 3 equiv of triethylamine and 1.5 equiv of 2-aminoethanthiol chloride were used, and the product was recrystallized from a *n*-hexane/CH_2Cl_2 mixture. ^{1}H NMR ($CDCl_3$, 250 MHz): $\delta = 0.88$(t, 3H; $C\underline{H}_3-[CH_2]_{14}-$), 1.25(br m, 28H; $CH_3-[C\underline{H}_2]_{14}-$), 1.63(m, 2H; $-C\underline{H}_2CH_2CONH-$), 2.19(t, 2H; $-CH_2C\underline{H}_2CONH-$), 2.66(br s, 1H; OH), 3.46(q, 2H; $-CONHC\underline{H}_2CH_2OH$), 3.75(m, 2H; $-CONHCH_2C\underline{H}_2OH$), 5.91(br s, 1H; $-CON\underline{H}-$); ESI-MS: *m*/*z*: 344.52 [M^+ + H], 366.54 [M^+ + Na], 342.39[M^- − H]. Silica gel TLC, ethyl acetate:CH_2Cl_2 ratio of 1:9, $R_f = 0.5$.

2.1.7. Boc-L-alanine(d_4). Boc-L-alanine(d_4) was prepared according to Itoh et al.[18] ^{1}H NMR ($CDCl_3$, 250 MHz): δ = 1.45(s, 9H), 6.55(s, 1H; −CONH−), 7.65(br s, 1H; −COOH); ESI-MS: *m*/*z*: 192.08 [M^- − H].

2.1.8. *p*-Octadecyl-phenol (C_{18}-PhOH). *p*-Octadecyl-phenol (C_{18}-PhOH) was prepared according to Hanabusa et al.[10] ^{1}H NMR ($CDCl_3$, 250 MHz): $\delta = 0.88$(t, 3H; $C\underline{H}_3$), 1.25(br m, 30H; $[C\underline{H}_2]_{15}$), 1.56(m, 2H; $-C\underline{H}_2CH_2Ph$), 2.52(t, 2H; $-CH_2-C\underline{H}_2Ph$), 4.68(s, 1H; $-PhO\underline{H}$), 6.75/7.04(double d, 4H; aromatic hydrogen); ESI-MS: *m*/*z*: 369.51[M^+ + Na], 385.52[M^+ + K], 354.34[M^- − H]. Silica gel TLC, 10% ethyl acetate in *n*-hexane, $R_f = 0.28$.

2.1.9. D-Alanine *p*-Octadecyl-phenyl Ester Trifluoroacetate Salt (Ala-C_{18}-Ph). Esterification of the D-alanine *p*-octadecyl-phenyl ester trifluoroacetate salt (Ala-C_{18}-Ph) was accomplished by following the method of Neises and Steglich.[19] *p*-Octadecyl-phenol (0.080 g, 0.19 mmol, 1 equiv), Boc-D-alanine (0.036 g, 0.19 mmol, 1 equiv), and DCC (0.060 g, 0.28 mmol, 1.5 equiv) were placed in a 25-mL round-bottom flask that was equipped with a magnetic stirring bar and a drying tube. The materials were dissolved in 10 mL of CH_2Cl_2 through the application of gentle heat, and the solution was placed over an ice-water bath. White material precipitated, and the solution was further cooled for 10 min. *N*,*N*-dimethyl 4-amino pyridine (0.0023 g, 0.019 mmol, 0.1 equiv) dissolved in a small amount of CH_2Cl_2 was added to the stirring mixture. The reaction was continued for 1 h at 0 °C, and then the ice was allowed to melt and the reaction was continued for another hour. The white precipitate (DCU) was filtered off and 100 mL of CH_2Cl_2 were added to the solution. The solution was washed with 0.5 M HCl (10 mL, 2 times) and sodium bicarbonate (20 mL, 2 times), dried with magnesium sulfate, and the solvent evaporated. The resulting material was transferred into a 10-mL round-bottom flask equipped with a drying tube and a magnetic stirring bar. The flask was placed over an ice-water bath, and 3 mL of CH_2Cl_2 and 5 mL of trifluoroacetic acid were added. The solution was stirred for 1 h and then the solvent was evaporated by bubbling

air through the solution. Another portion of CH_2Cl_2 was added and evaporated in the same manner. The remaining oil was transferred to high vacuum for 1 h, and then diethyl ether was added (7 mL); the oil was dissolved and, after a short time, a white material precipitated. The mixture was kept at a temperature of 4 °C overnight and the precipitate was filtered, washed with 10 mL of diethyl ether, recrystallized from a *n*-hexane/CH_2Cl_2 mixture, and dried in a vacuum to give 0.080 g (80% yield) of pure Ala-C_{18}-Ph. ^{1}H NMR (5%CD_3OD in $CDCl_3$, 250 MHz): $\delta = 0.88$(t, 3H; $C\underline{H}_3-[CH_2]_{15}-$), 1.25(br m, 30H; $CH_3-[C\underline{H}_2]_{15}-$), 1.60(m, 2H; $-C\underline{H}_2CH_2Ph-$), 1.70(d, 3H; $-CHC\underline{H}_3-NH_3^+$), 2.60(t, 2H; $-CH_2C\underline{H}_2Ph-$), 4.22(q, 1H; $-C\underline{H}CH_3-NH_3^+$), 6.99/7.19(double d, 4H; aromatic H); ESI-MS: *m*/*z*: 418.52[M^+ + H], 440.53[M^+ + Na].]. Silica gel TLC, ethanol/CH_2Cl_2 ratio of 1:9, $R_f = 0.4$.

Note: All of the following materials were synthesized in the same manner as Ala-C_{18}-Ph from the corresponding alcohols or thio-alcohols and *N*-Boc protected amino acids.

2.1.10. D- and DL-Alanine Octadecanamid-*N*-Ethyl Ester Trifluoroacetate Salt (Ala-C_{18}-AE). ^{1}H NMR (5% CD_3OD in $CDCl_3$, 250 MHz): $\delta = 0.88$(t, 3H; $C\underline{H}_3-[CH_2]_{14}-$), 1.25(br m, 28H; $CH_3-[C\underline{H}_2]_{14}-$), 1.57(br d, 5H; $-CHC\underline{H}_3NH_2$; $-C\underline{H}_2-CH_2CONH-$), 2.16(t, 2H; $-CH_2C\underline{H}_2CONH-$) 3.50(m, 2H; $-CONHC\underline{H}_2CH_2O-$), 4.04(q, 1H; $-C\underline{H}CH_3NH_2$), 4.1−4.4(br m, 2H; $-CONHCH_2C\underline{H}_2O-$), 6.77(t, 1H; $-CON\underline{H}-$); ESI-MS: *m*/*z*: 399.55[M^+ + H], 421.55[M^+ + Na].

2.1.11. L-Alanine(d_4) Octadecanamid-*N*-ethyl Ester Trifluoroacetate Salt (Ala-C_{18}-AE). ^{1}H NMR ($CDCl_3$, 400 MHz): $\delta = 0.88$(t, 3H; $C\underline{H}_3-[CH_2]_{14}-$), 1.26(br m, 28H; $CH_3-[C\underline{H}_2]_{14}-$), 1.58(m, 2H; $-C\underline{H}_2CH_2CONH-$), 2.17(t, 2H; $-CH_2C\underline{H}_2-CONH-$) 3.51(m, 2H; $-CONHC\underline{H}_2CH_2O-$), 4.15−4.35(br m, 2H; $-CONHCH_2C\underline{H}_2O-$), 6.68(m, 1H; $-CON\underline{H}-$); ESI-MS: *m*/*z*: 403.82[M^+ + H], 425.86[M^+ + Na].

2.1.12. D- and DL-Alanine Octadecanamid-*N*-ethyl Thioester Trifluoroacetate Salt (Ala-C_{18}-ATE). ^{1}H NMR (5% CD_3OD in $CDCl_3$, 250 MHz): $\delta = 0.88$(t, 3H; $C\underline{H}_3-[CH_2]_{14}-$), 1.25(br m, 28H; $CH_3-[C\underline{H}_2]_{14}-$), 1.61(m, 5H; $-CHC\underline{H}_3NH_2$; $-C\underline{H}_2-CH_2CONH-$), 2.16(t, 2H; $-CH_2C\underline{H}_2CONH-$), 2.9−3.2(br m, 2H; $-CONHCH_2C\underline{H}_2S-$), 3.39(m, 2H; $-CONHC\underline{H}_2CH_2S-$), 4.13(q, 1H; $-C\underline{H}CH_3NH_2$), 6.68(t, 1H; $-CON\underline{H}CH_2CH_2S-$); ESI-MS: *m*/*z*: 415.61 [M^+ + H], 437.59 [M^+ + Na]. Silica gel TLC, ethanol/CH_2Cl_2 ratio of 1:9, $R_f = 0.5$.

2.1.13. L-Alanine(d_4) Octadecanamid-*N*-ethyl Thioester Trifluoroacetate Salt (Ala-C_{18}-ATE). ESI-MS: *m*/*z*: 419.74[M^+ + H], 441.71[M^+ + Na].

2.1.14. D- and L-Serine Octadecanamid-*N*-ethyl Thioester Trifluoroacetate Salt (Ser-C_{18}-ATE). ^{1}H NMR ($CDCl_3$, 400 MHz): $\delta = 0.82$(t, 3H; $C\underline{H}_3-[CH_2]_{14}-$), 1.25(br m, 28H; $CH_3-[C\underline{H}_2]_{14}-$), 1.71(m, 2H; $-C\underline{H}_2CH_2CONH-$), 2.60(t, 2H; $-CH_2-C\underline{H}_2CONH-$), 3.33(m, 2H; $-CONHCH_2C\underline{H}_2S-$), 3.76(t, 2H; $-CONHC\underline{H}_2CH_2S-$), 4.42(br m, 2H; $-C\underline{H}_2OH$), 4.67(m, 1H; $-C\underline{H}NH_3^+-$); *m*/*z*: 431.79[M^+ + H], 453.76[M^+ + Na].

2.2. GIXD Measurements. GIXD measurements were performed using the liquid-surface diffractometer at the BW1 synchrotron beamline at HASYLAB, DESY facility in Hamburg, Germany. Details about the experimental technique and the instrument were reported elsewhere.[20] The measured GIXD patterns are represented as 2D contour maps presenting the scattered intensity ($I(q_{xy}, q_z)$) as a function of the horizontal (q_{xy}) and vertical (q_z) components of the scattering vector. The unit cell dimensions of the 2D lattice are derived from the q_{xy} positions of the Bragg peaks. The full width at half-maximum of the Bragg peaks (corrected for instrument resolution), fwhm(q_{xy}), gives the crystalline coherence lengths $L_{hk} \approx 0.9(2\pi/\text{fwhm}(q_{xy}))$ associated with each *h*,*k* reflection. Bragg rod intensity profiles are the intensity distribution along q_z, $I(q_z)$, derived by integrating across the q_{xy} range for each of the Bragg peaks. The full width at half-maximum of the Bragg rod intensity profiles, fwhm(q_z), gives a first estimate of the thickness of the 2D crystallites: $L_z \approx 0.9(2\pi/\text{fwhm}(q_z))$. For chainlike molecules, such as aliphatic hydrocarbons, precise information on the molecular chain orientation in 2D crystals may be obtained from the positions of the maxima of Bragg rods, if the chains are uniformly tilted. The tilt angle *t* between the molecular axis and the surface normal is given by the equation[21,22]

$$\cos\psi_{hk}\tan t = \frac{q_z^0}{|\boldsymbol{q}_{hk}|}$$

where q_z^0 is the position of the maximum along the Bragg rod and ψ_{hk} is the azimuthal angle between the chain tilt direction projected onto the *xy*-plane and the reciprocal vector $\boldsymbol{q}_{hk}$. More accurately, the intensity at a particular value of q_z in a Bragg rod is determined by the square of the molecular structure factor, $|\boldsymbol{F}_{h,k}(q_z)|^2$. The 2D packing arrangements were determined by performing X-ray structure factor calculations, using atomic coordinate molecular models constructed using the CERIUS^2 molecular package,[23] and rigid-body structure refinement, using the SHELX-97 program[24] adapted for 2D structures.

2.3. Polymerization Experiments. The materials were dissolved in chloroform, benzene, or chloroform with 4% methanol to give a solution concentration of 0.5 mM. The solution was spread on the subphase to the desired area per molecule and allowed to react for different periods of time, from a few minutes up to 20 h (see Table 1). The subphase for the different compounds were as follows: pure water; 0.01 M phosphate buffer, pH 8.0 (3.4 mL of 1 M NaH_2PO_4 + 183 mL of 0.2 M Na_2HPO_4 into 4 L of water); 1 mM or 0.1 mM copper chloride ($CuCl_2$); 0.01 M carbonate/bicarbonate buffer, pH 10.0 (88 mL of 0.2 M Na_2CO_3 + 112 mL of 0.2 M $NaHCO_3$ into 4 L of water). In some cases, the material was spread on pure water and then copper chloride was injected from a concentrated solution to give the desired final concentration; for example, 1 mM (50 mL of 28 mM injected into 1350 mL (the trough volume)). In these cases, the chloroform was allowed to evaporate for 10−15 min prior to the injection of the catalyst.

2.4. MALDI−TOF MS. After the reaction, the monolayer films were compressed with the barrier and the material was collected from the liquid surface, transferred to a glass vial, and dried by a stream of dry nitrogen. Samples for the MALDI−TOF MS analysis were then prepared by dissolving the dry material in chloroform containing 5% trifluoroacetic acid. A small amount (0.5 μL) of this solution was deposited on top of a matrix deposit (1:1 v:v of dithranol solution in chloroform and NaI saturated solution in tetrahydrofuran (THF)) on the instrument holder. The MALDI−TOF positive-ion mass spectra were obtained in reflector mode from two different instruments at the Weizmann Institute (Bruker Reflex III) that were equipped with a N_2 laser. External calibration of the mass spectra was achieved using a calibrating peptide (Substance P, ACTH 8-39) in the studied mass range. Only singly charged ions, $(M + H)^+$ and $(M + Na)^+$ with the expected isotopic pattern, were observed. Mass spectra resulted from a signal average of at least a few hundred laser shots in different spots of the target to get reliable statistics about the ion peak. Good statistics are obtained when the isotopic distribution of an ion species corresponds to that expected from calculation. Mass assignments were made using both *m*/*z* measurement and isotopic distribution.

TABLE 1: Experimental Conditions for Polymerization Experiments

material[a]	solvent[b]	mean area, M_a (Å^2)[c]	duration	temperature, T (°C)	catalyst
Ala-C_{18}	1, 3	25, 28[d]	10 min, 3 h, 5 h	20	water, pH 8, $CuCl_2$ 1 mM
Ala-C_{26}-TFA[e]	1	35	20 h	20	water
Phe-C_{18}	1	49	3 h	20	$CuCl_2$ 1 mM
Tyr-C_{18}	1	38,35	10 min, 3 h, 5 h	20	$CuCl_2$ 1 mM
Ala-C_{18}-AE-TFA[e]	2	35	10 min, 2.5 h	20	$CuCl_2$ 1 mM[f]
Ala-C_{18}-ATE-TFA[e]	2	35	10 min, 3 h	3	$CuCl_2$ 0.1 mM[f]
Ala-C_{18}−Ph-TFA[e]	1	35	10 min, 3.5 h	20	water
Ser-C_{18}-ATE-TFA[e]	2	35	10 min, 2.5 h	3	water
Glu-$(C_{18})_2$	1	45	3 h	3	$CuCl_2$ 1 Mm
Glu-$(C_{18})_2$-MSA[g]	1	45	3 h, 24 h	30	water, pH 10

[a] See Scheme 1. [b] The solvents are as follows: 1, chloroform; 2, chloroform/4% methanol; and 3, benzene. [c] The mean area per molecule over which the material was spread. [d] The material was spread over an area of 30 Å^2/molecule and compressed to 28 or 25 Å^2/molecule. [e] The material was spread on the surface as a salt with trifluoroacetic acid. [f] A concentrated catalyst solution was injected under the monolayer to achieve the reported final concentration. [g] The material was spread as a salt of methyl-sulfonic acid.

SCHEME 2: Molecular Formulas of the Monomers Investigated

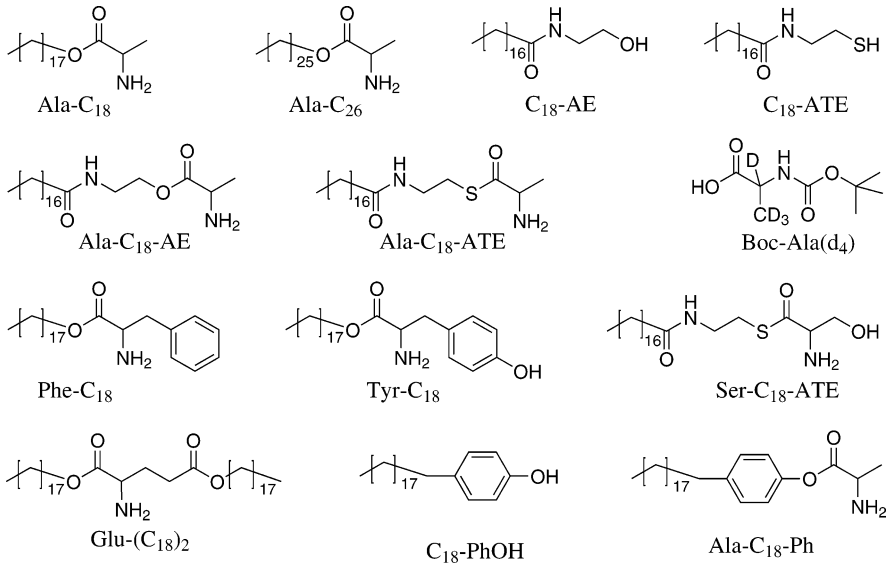

We use the following notation code for the oligopeptide molecules: (*h*,*d*) designates a molecule comprising *h* D-(protonated) repeat units and *d* L(deuterated) repeat units, with $n = h + d$, being the total number of repeat units. The relative abundance (r.a.) of each type of oligopeptide (*h*,*d*) is obtained by dividing the intensity of all the ions from a particular molecule to the total intensity of the ions from all the molecules of the same length, *n*. For example, the relative abundance of a tetrapeptide (4,0) which is composed of four (protonated) D-alanine molecules, is calculated from the equation

$$\text{r.a.}(4,0) = \frac{\text{Intensity}(4,0)}{\text{Intensity}\{(4,0) + (3,1) + (2,2) + (1,3) + (0,4)\}}$$

The relative abundance of the tetrapeptide (2,2), which is composed of two (protonated) D-alanine molecules and two (deuterated) L-alanine molecules is calculated from the equation

$$\text{r.a.}(2,2) = \frac{\text{Intensity}(2,2)}{\text{Intensity}\{(4,0) + (3,1) + (2,2) + (1,3) + (0,4)\}}$$

The ionization yield is expected to be very similar for the (*h*,*d*) oligopeptides of the same length $n = h + d$. In view of the very similar masses of the compounds and the resulting very similar ion velocities in the TOF mass spectrometer, we may assume similar detection efficiencies.[25] Thus, the ion intensity of the different (*h*,*d*) oligopeptides are directly and reliably comparable.

3. Results and Discussion

3.1. Ala-C_{18} and Ala-C_{26}. The first system we investigated was Ala-C_{18} (Scheme 2). The GIXD patterns measured from monolayers of DL- and L-Ala-C_{18} are shown in Figure 1a and 1b, respectively, as 2D contour plots of intensity $I(q_{xy},q_z)$, as a function of the horizontal q_{xy} and vertical q_z components of the scattering vector. A relatively strong diffraction was obtained at a mean molecular area of 28 and 24 Å^2 (Figure 2). At this surface coverage, the reported polymerization reaction was optimal.[9] At lower surface coverage, the diffraction intensity was very weak. Assignment of the (*h*,*k*) Miller indices to the GIXD pattern measured from DL-Ala-C_{18} yielded a rectangular unit cell ($a = 5.0$ Å, $b = 10.5$ Å, $A_m = 26$ Å^2; see Table 2) that contained two molecules whose hydrocarbon chains are tilted along the *b*-axis by an angle of 40° from the normal to the water surface (calculated from the q_z position of the maximum intensity of the Bragg rods;[21,22] see Experimental Section). The unit cell has typical dimensions for a herringbone packing motif of the two molecules that are related by glide symmetry along the *b*-axis. The GIXD pattern measured from L-Ala-C_{18} was assigned according to an oblique subcell ($a_o = 5.0$ Å, $b_o = 5.4$ Å, $\gamma_o = 115.5°$, $A_m = 24$ Å^2) that can be transformed into a cell with almost rectangular (pseudo-rectangular) dimensions: $a_r = 5.0$ Å, $b_r = 9.8$ Å, $\gamma_r = 91.7°$, $A_m = 24$ Å^2. The latter contains two independent molecules whose hydrocarbon chains are related by pseudo-glide almost parallel to the *b*-axis. Note

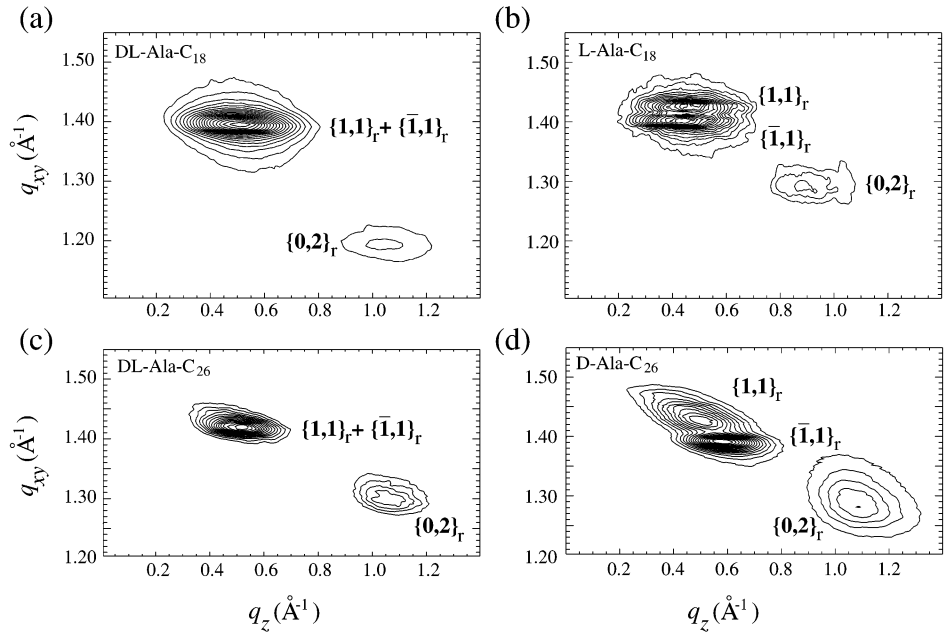

Figure 1. GIXD patterns $I(q_{xy},q_z)$ measured from the two-dimensional (2D) crystallites of (a) DL-Ala-C_{18} and (b) L-Ala-C_{18} at a mean molecular area of 24 Å^2 and (c) DL-Ala-C_{26} and (d) D-Ala-C_{26} at a mean molecular area of 35 Å^2.

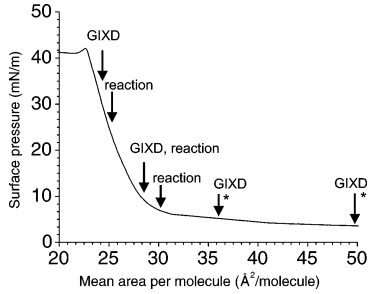

Figure 2. Surface pressure−mean molecular area isotherm of DL-Ala-C_{18} at 20 °C, showing the points where GIXD and polycondensation reactions were performed. No diffraction was obtained at the points marked with an asterisk, * (at 50 and 36 Å^2/molecule).

that the GIXD patterns measured from the two-dimensional (2D) crystallites of DL- and L-Ala-C_{18} are significantly different from that measured for the octadecanol precursor,[26] indicating that the two 2D packing arrangements are dependent on the chiral alanine moiety.

Polymerization experiments performed using DL- and L-Ala-C_{18} spread over a mean molecular area of 30 Å^2 and compressed to 28 or 25 Å^2 yielded only dimers, as determined by MALDI−TOF MS analysis of samples taken from the water surface. A possible reason for this result could be the lower tendency of these molecules to form ordered crystallites. Therefore, we investigated Ala-C_{26} (Scheme 2), which we expected to self-assemble on the water surface into 2D domains with a higher degree of order, because of stronger interactions between the longer hydrocarbon chains.[26] Indeed, the GIXD patterns measured from DL- and D-Ala-C_{26}, spread over a surface coverage of only 70% (mean molecular area of 35 Å^2), showed a strong diffraction (see Figure 1c, d). The racemic DL-Ala-C_{26} packs in a rectangular unit cell ($a = 5.0$ Å, $b = 9.6$ Å, $A_m = 24$ Å^2) that contains two molecules tilted along the *b*-axis by an angle of 39° from the normal to the water surface. The molecules are related by a *b*-glide symmetry in a herringbone packing motif as racemic 2D crystallites. To determine the 2D packing arrangement, X-ray structure factor calculations were performed with the Shelx97[24] program adapted for 2D crystals. Using an atomic coordinate molecular model, the structure was refined to obtain a reasonable fit between the measured and calculated Bragg rod intensity profiles (Figure 3a). The refined 2D packing arrangement is shown in Figure 3b, viewed perpendicular to the water surface.

The GIXD pattern (Figure 1d) measured from D-Ala-C_{26} was analyzed in terms of a pseudo-rectangular unit cell ($a = 5.0$ Å, $b = 9.8$ Å, $\gamma = 92.0°$, $A_m = 24$ Å^2) that contains two molecules related by a pseudo-glide plane along the *b*-axis. The refined model that best fitted the Bragg rod intensity profiles (Figure 3c) is shown in Figure 3d, viewed perpendicular to the water surface.

Polymerization experiments performed with D- and DL-Ala-C_{26} at 35 and 25 Å^2/molecule showed that the higher degree of crystalline order did not contribute to the formation of longer oligopeptides and, again, only dimers were obtained, according to the MALDI−TOF MS analysis.

3.2. Ala-C_{18}-AE. According to the GIXD results, DL-Ala-C_{18} and DL-Ala-C_{26} pack in a racemic plane group containing both enantiomers in the same crystallite. In such systems, the polymerization can occur between either homochiral or heterochiral molecules, depending on the molecular arrangement, distance, and orientation of neighboring D−D versus D−L pairs. A simpler way to obtain homochiral peptides would be when racemic monomers separate on the water surface into a mixture of enantiomorphous domains, each containing molecules of a single-handedness. To achieve such a separation, we introduced an amide group into the hydrocarbon chain because, as shown previously,[27] this group can promote hydrogen bonding between molecules related by translation, thus enhancing the possibility of spontaneous separation of the racemate into a mixture of enantiomorphous domains.

Ala-C_{18}-AE (Scheme 2) contains an amide group separated by a $-(CH_2)_2-$ "spacer" from the alanine-ester moiety. GIXD patterns measured from self-assembled 2D crystallites of DL- and D-Ala-C_{18}-AE are presented in Figure 4a and b, respectively. For comparison, a significantly different GIXD pattern was measured from self-assembled 2D crystallites of the C_{18}-AE precursor alcohol (Scheme 2), as shown in Figure 4c. Initially, an attempt was made to index the GIXD pattern of DL-Ala-C_{18}-AE, according to a pseudo-rectangular unit cell ($a_r = 4.9$

TABLE 2: Unit Cell Dimensions and Molecular Tilt Angles, as Deduced from the GIXD Measurements at the Air/Water Interface

											Coherence Length, L_{hk} (Å)[h]		
material[a]	M_a (Å)[b]	a_o (Å)[c]	b_o (Å)[c]	γ_o (°)[c]	a_r (Å)[d]	b_r (Å)[d]	γ_r (°)[d]	A_m (Å^2)[e]	t (°)[f]	ψ_a (°)[g]	L_{01}	L_{10}	$L_{\bar{1}1}$
L-Ala-C_{18}	24	5.0	5.4	115.5	5.0	9.8	91.7	24	35	91	140	170	180
DL-Ala-C_{18}	24				5.0	10.5	90	26	40	90	100[i]	140[i]	
D-Ala-C_{26}	35	5.0	5.4	115.4	5.0	9.8	92.0	24	40	95	100	260	110
DL-Ala-C_{26}	35				5.0	9.6	90	24	39	90	140[i]	240[i]	
D-Ala-C_{18}-AE	29	4.9	5.4	115.8	4.9	9.8	90.9	24	37	93	250	500	320
DL-Ala-C_{18}-AE	29	4.9	5.4	115.0	4.9	9.9	91.8	24	37	80	130	340	300
L-Ala-C_{18}-ATE	29	4.9	5.4	113.8	4.9	9.9	93.2	24	38	79	160	280	320
DL-Ala-C_{18}-ATE	29	4.9	5.4	113.8	4.9	9.9	93.2	24	38	79	170	280	280
L-Ala-C_{18}−Ph	35	5.1	5.3	113.9	5.1	9.8	94.7	25	36	85	120	250	230
DL-Ala-C_{18}−Ph	35	5.1	5.3	112.6	5.1	9.8	96.3	25	37	88	110	120	90
D-Ser-C_{18}-ATE	35	4.9	5.4	114.2	4.9	9.9	92.9	24	39	79	250	450	310
DL-Ser-C_{18}-ATE	35				4.9	9.1	90	22	33	90	400[i]	500[i]	
L-Glu-$(C_{18})_2$	55				5.0[j]	8.6[j]	90	43[j]	25	0	340[i]	80[i]	
DL-Glu-$(C_{18})_2$	55				5.0[j]	8.6[j]	90	43[j]	25	0	340[i]	70[i]	
DL-Glu-$(C_{18})_2$[k]	45				5.0[j]	8.3[j]	90	42[j]	18	90	80[i]	110[i]	
C_{18}-AE	29				4.9	9.0	90	22	32	90	470[i]	560[i]	
C_{18}-ATE	29				4.9	9.0	90	22	32	90	410[i]	510[i]	
C_{18}−PheOH	35				5.1	9.0	90	23	32	90	510[i]	560[i]	
hexacosanol	35				5.0	7.4	90	18	7	90	420[i]	360[i]	

[a] Chirality is as indicated. [b] Mean area per molecule at which the diffraction was measured. [c] Oblique unit cell parameters. [d] Rectangular or pseudo-rectangular unit cell parameters calculated from the oblique cell with $a_r = -a_o$ and $b_r = a_o + 2b_o$. [e] Area per molecule calculated from the diffraction data. [f] Molecular tilt angle from the normal to the water plane. [g] Azimuthal angle between the projection of the long molecular axes on the water plane and the *a*-axis of the unit cell (as $a_r = -a_o$, this is the same angle for the rectangular and oblique unit cells). [h] As deduced from the full width at half maximum, $\text{fwhm}_{(h,k)}$. [i] L_{02} and $L_{11+\bar{1}1}$, respectively. [j] Rectangular subcell containing one molecule. [k] Subphase is 1 mM $CuCl_2$.

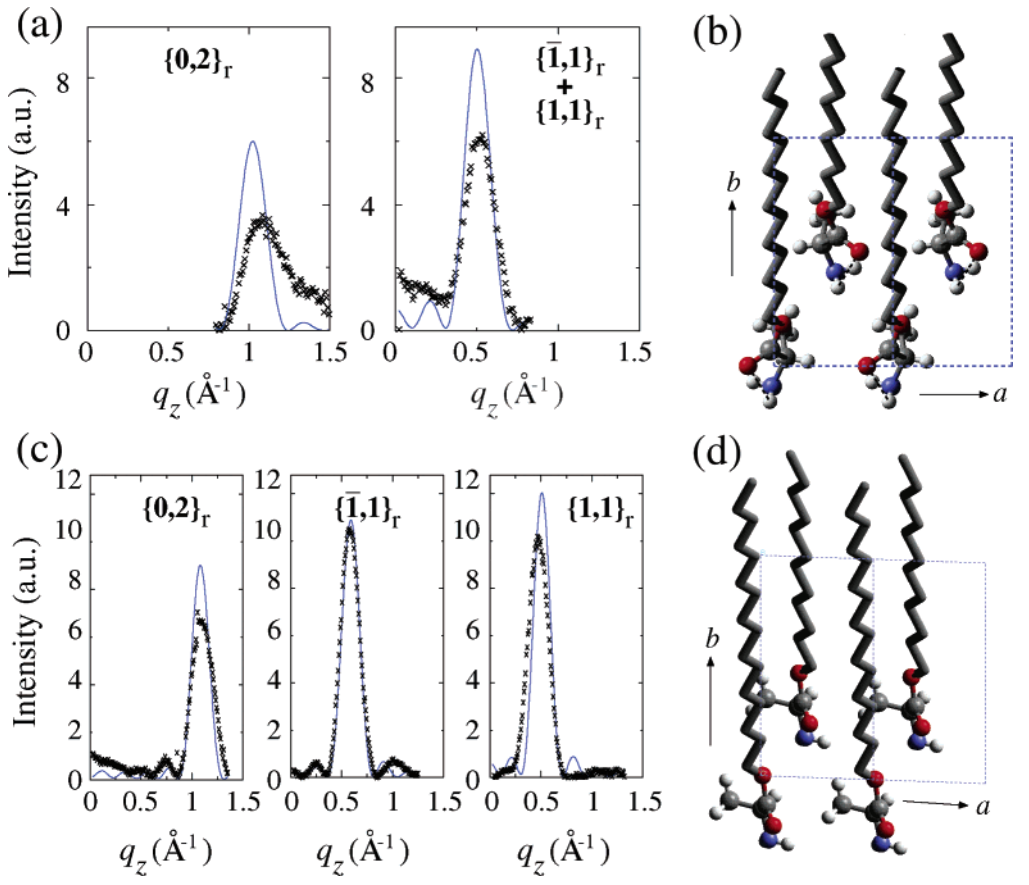

Figure 3. (a) Bragg rod intensity profiles ((×) measured and (—) calculated) and (b) the refined 2D packing arrangements (viewed perpendicular to the water surface) of DL-Ala-C_{26}; (c) Bragg rod intensity profiles ((×) measured and (—) calculated) and (d) the refined 2D packing arrangements (viewed perpendicular to the water surface) of D-Ala-C_{26}. Note that, for clarity, only portions of the hydrocarbon chains are shown.

Å, $b_r = 9.9$ Å, $\gamma_r = 91.8°$, $A_m = 24$ Å^2) that contained two molecules. The calculated molecular tilt angle is 37° from the normal to the water surface in an azimuth angle of 12° from the *b*-axis. However, this unit cell cannot accommodate two molecules that are related by a pseudo-glide, because the tilt direction is not along a crystallographic axis. The tilt direction

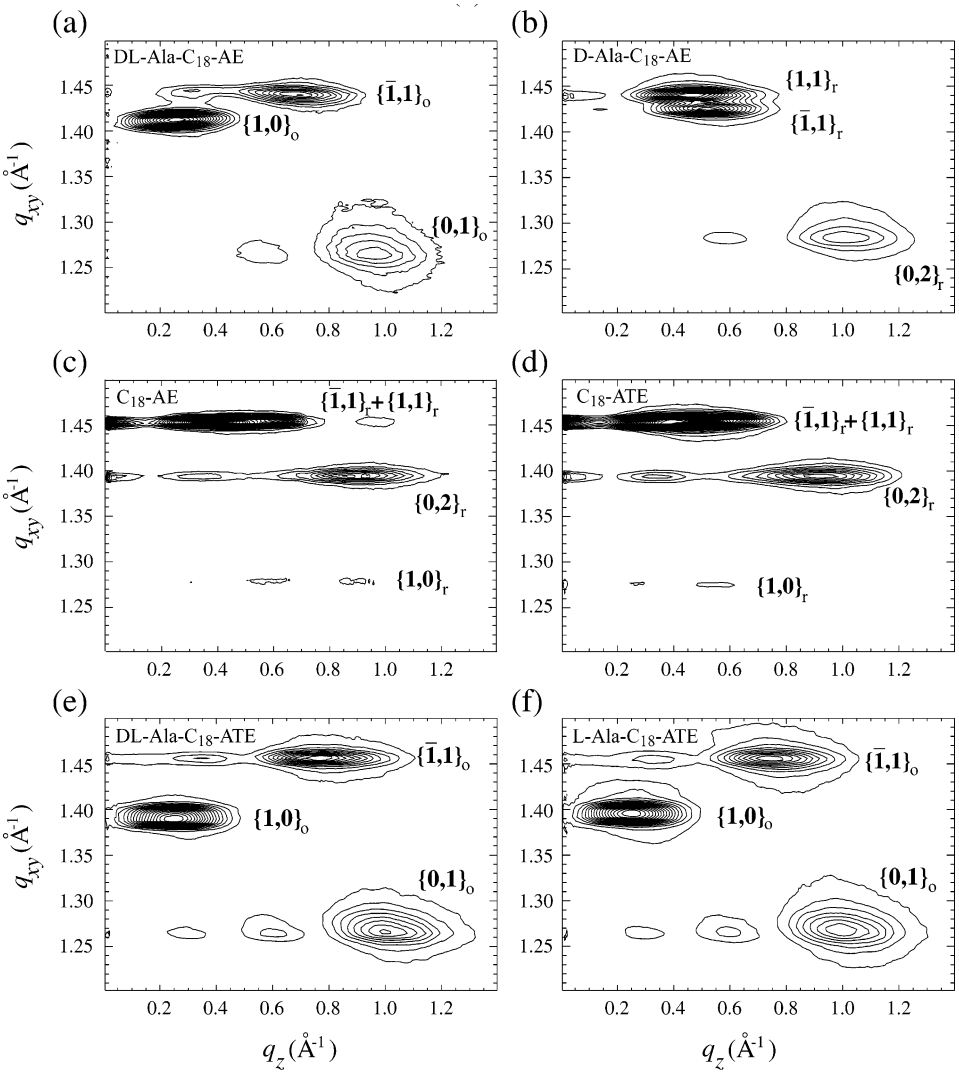

Figure 4. GIXD patterns $I(q_{xy},q_z)$ measured at a mean molecular area of 29 Å^2 from the 2D crystallites of (a) DL-Ala-C_{18}-AE, (b) D-Ala-C_{18}-AE, (c) C_{18}-AE, (d) C_{18}-ATE, (e) DL-Ala-C_{18}-ATE, and (f) L-Ala-C_{18}-ATE.

indicates that Ala-C_{18}-AE molecules can be related by translation symmetry in the corresponding chiral oblique subcell, of dimensions $a_o = 4.9$ Å, $b_o = 5.4$ Å, $\gamma_o = 115.0°$. The proposed 2D packing arrangement is presented in Figure 5b together with the calculated and measured Bragg rods intensity profiles (Figure 5a). In such a molecular arrangement, we can envisage enantiomeric disorder within the chiral domains via an interchange between the CH_3 group and the H atom at the stereogenic carbon to yield a random solid solution of the two enantiomers. Polymerization experiments of DL-Ala-C_{18}-AE at 20 °C for 2.5 h, initiated by an aqueous solution of $CuCl_2$ (1 mM), yielded only a mixture of diastereoisomeric dipeptides, as determined by MALDI−TOF MS analysis of samples prepared using an L-enantiomer with deuterated L-Ala(d_4) (see Experimental Section). The experimental relative abundance of each of the dipeptides is given in Figure 6a, in comparison to the theoretical values expected for a random polymerization process. The composition of the three diastereoisomeric dipeptides follows a binomial distribution, as would be expected for self-assembly of the DL-Ala-C_{18}-AE into a random 2D solid solution. We also note that the GIXD pattern of D-Ala-C_{18}-AE (Figure 4b) is different.

The GIXD diffraction pattern[28] of D-Ala-C_{18}-AE (Figure 4b) was indexed according to a pseudo-rectangular unit cell (a = 4.9 Å, b = 9.8 Å, $\gamma = 90.9°$, $A_m = 24$ Å^2) that contained two molecules, tilted by 37° from the normal to the water surface, in a direction almost parallel to the b-axis. This tilt direction indicates that hydrocarbon chains can pack in a pseudo-herringbone packing motif via a pseudo-glide plane whereas the Ala-headgroups are related by pseudo-translation. The 2D molecular packing arrangement, determined by X-ray-structure-factor-constrained least-squares refinement, is shown in Figure 5c, together with the calculated and measured Bragg rods profiles (Figure 5d).

3.3. Ala-C_{18}-ATE. The polymerization of the alanine long-chain esters described previously yielded only dipeptides. We expected that longer oligopeptides should be obtained using the more-reactive corresponding thio-esters. For this purpose, Ala-C_{18}-ATE (Scheme 2, as trifluoroacetate salt) was investigated. The GIXD patterns measured from the 2D crystallites self-assembled from DL- and L-Ala-C_{18}-ATE at a mean area of 29 Å^2/molecule (Figure 4e, f) are very different from the GIXD pattern (Figure 4d) measured from the corresponding C_{18}-ATE thio-alcohol precursor is isostructural to C_{18}AE. The diffraction patterns in Figure 4e and f are very similar, indicating that the Ala-C_{18}-ATE racemate might have spontaneously separated into a mixture of enantiomorphous 2D domains. The diffraction patterns were both indexed according to an oblique cell (a = 4.9 Å, b = 5.4 Å, $\gamma = 113.8°$, $A_m = 24$ Å^2). The molecules are tilted by 38° from the normal to the water surface, with an

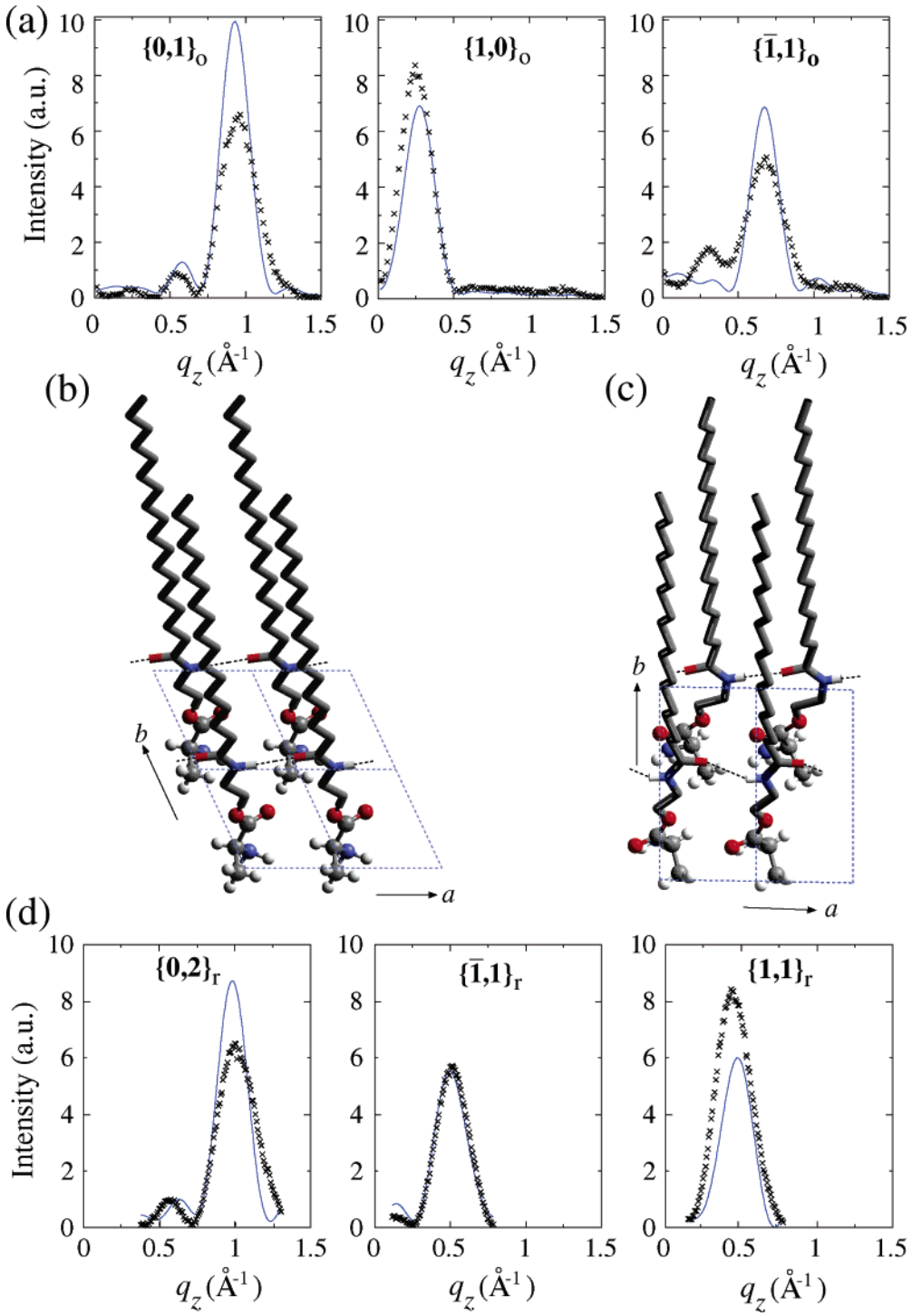

Figure 5. (a) Bragg rod intensity profiles of DL-Ala-C_{18}AE ((×) measured and (—) calculated); (b) refined 2D packing arrangements of DL-Ala-C_{18}AE, viewed perpendicular to the water surface; (c) refined 2D packing arrangements of D-Ala-C_{18}AE, viewed perpendicular to the water surface; and (d) Bragg rod intensity profiles of D-Ala-C_{18}AE ((×) measured and (—) calculated).

azimuthal direction of 79° from the *a*-axis. X-ray-structure-factor-constrained least-squares refinement of the atomic coordinate model yielded the 2D packing arrangement given in Figure 7b, together with the Bragg rod intensity profiles (Figure 7a).

MALDI−TOF MS of samples collected from the aqueous surface after 3 h on a 1 mM $CuCl_2$ subphase at 4 °C revealed the formation of a mixture of diastereoisomeric dipeptides, tripeptides, and tetrapeptides. The experimental relative abundance of each of the oligopeptides is given in Figure 6b and compared with the theoretical binomial distribution expected for a random process. Note that the dimer gave the strongest signals in the MALDI−TOF MS analysis, whereas the intensities of the trimer, unreacted monomer, and tetramer were in a descending order (Figure 6c). The experimental results are very close to the binomial distribution in a random process, indicating the occurrence of enantiomeric disorder in the 2D crystallites self-assembled from the racemate. Such disorder can occur via an interchange of the methyl group with the H atom attached to the asymmetric C atom. This type of disorder cannot be determined on the basis of our GIXD data. Another possibility may be that the polymerization reaction occurred primarily at the grain boundaries or in the amorphous portion of the monolayer and not within the 2D crystallites.

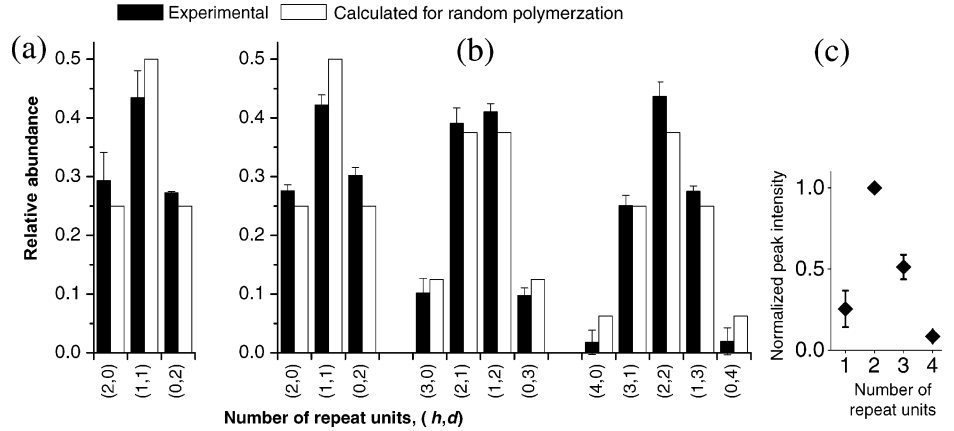

Figure 6. Relative abundance of oligopeptides obtained at the air/water interface, as determined by MALDI−TOF MS using deuterium-labeled L-monomer: (a) Ala-C_{18}-AE (35 Å^2/molecule, 10 mM $CuCl_2$, 4 °C, 3 h) and (b) Ala-C_{18}-ATE (1 mM $CuCl_2$, 4 °C, 3 h), average of four independent samples. (c) MALDI−TOF MS peak intensity of the different oligopeptides and unreacted monomer as formed from the Ala-C_{18}-ATE normalized to that of the intensity of the dipeptide.

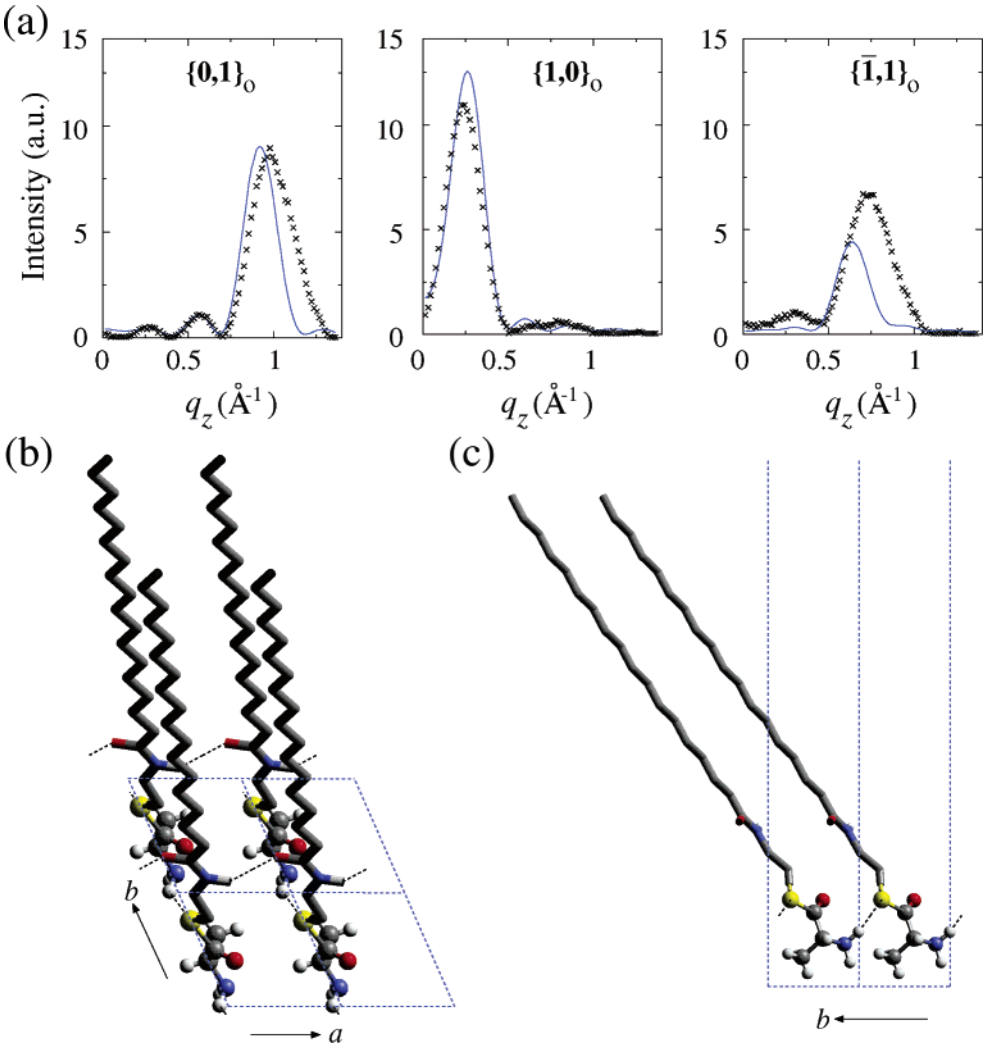

Figure 7. (a) Bragg rod intensity profiles of D-Ala-C_{18}-ATE 2D crystallites self-assembled from either D-or DL-amphiphiles ((×) measured and (—) calculated). Also shown are the refined packing arrangements of D-Ala-C_{18}-ATE 2D crystallites self-assembled from either D-or DL-amphiphiles, viewed (b) perpendicular and (c) parallel to the water surface.

3.4. Ala-C_{18}-Ph. Both Ala-C_{18}-AE and Ala-C_{18}-ATE were unsuitable for our purposes, because, apparently, both formed 2D crystallites comprising enantiomeric disorder. Nevertheless, the introduction of a thio-ester moiety in Ala-C_{18}-ATE increased the length of the longest oligopeptide products obtained from two to four repeating units. To enhance the reactivity of the monomers, we used another reactive system exhibiting a phenyl ester as a good leaving group: Ala-C_{18}-Ph (Scheme 2). The GIXD patterns measured from the 2D crystallites self-assembled from DL-and L-Ala-C_{18}−Ph at a mean area of 35 Å^2/molecule are shown in Figure 8a and b, respectively. For comparison, the GIXD pattern measured from the corresponding C_{18}−PhOH

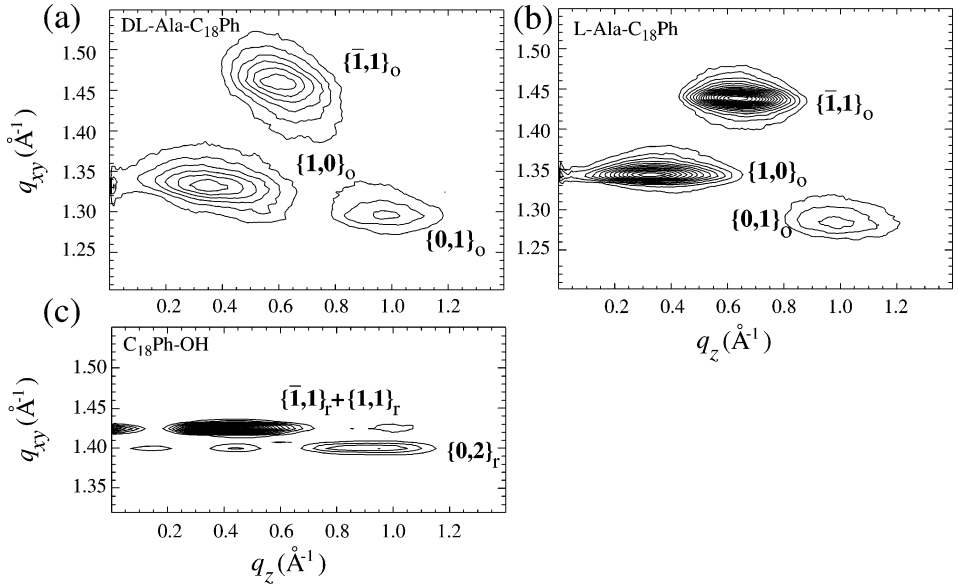

Figure 8. GIXD patterns $I(q_{xy},q_z)$ measured at a mean molecular area of 35 Å^2 from the 2D crystallites self-assembled from (a) DL-Ala-C_{18}Ph, (b) L-Ala-C_{18}Ph, and (c) C_{18}-PhOH.

(Scheme 2) alcohol precursor is very different (Figure 8c), demonstrating again that the packing arrangement of the alanine long-chain esters is dependent on the chiral alanine moiety. The diffraction pattern in Figure 8a was indexed according to a chiral oblique unit cell $a = 5.1$ Å, $b = 5.3$ Å, $\gamma = 112.6°$, $A_m = 25$ Å^2. The molecules are tilted by 37° from the normal to the water surface in an azimuthal direction of 88° from the *a*-axis. The GIXD data cannot give information on the degree of order of the alanine moieties in the crystallites. The unit cell of the L-crystallites (Figure 8b) are of similar dimensions to the racemate: $a = 5.1$ Å, $b = 5.3$ Å, $\gamma = 113.9°$, $A_m = 25$ Å^2. The 2D packing arrangement of the enantiomer L-crystallites is given in Figure 9, together with the measured and calculated Bragg rod intensity profiles. Polymerization performed on samples prepared from DL- and L-Ala-C_{18}-Ph yielded only dimers, as determined by MALDI−TOF MS analysis.

3.5. Phe-C_{18} and Tyr-C_{18}. The monomers derived from the alanine esters or thio-esters formed 2D crystallites comprising enantiomeric disorder. Such disorder would not be expected in systems where the α-amino acid side chain is bulky, e.g., Phe-C_{18} and Tyr-C_{18} (Scheme 2). Our polymerization experiments with these compounds, performed under the same conditions as previously reported[11,12] to yield oligopeptides in form of α-helix and/or random coil,[11,12] led to the formation of only dimers and unreacted monomer, as determined by MALDI−TOF MS analysis.

The GIXD measurements performed on monolayers of Phe-C_{18} and Tyr-C_{18} did not produce diffraction at any molecular area. The lack of crystalline order in such monolayers is presumably due to the steric hindrance introduced by the bulky Phe and Tyr headgroups.

3.6. Ser-C_{18}-ATE. Another system where we would expect the enantiomeric disorder to be reduced is the long-chain ester of serine Ser-C_{18}-ATE (see Scheme 2). The GIXD patterns measured from 2D crystallites self-assembled from DL- and L-Ser-C_{18}-ATE are given in Figure 10a and b, respectively. The L-crystallites display a diffraction pattern very similar to that of the Ala-C_{18}-ATE (see Figure 4e, f) with molecules packed only by translation. By contrast, the GIXD pattern measured from the racemic amphiphile yielded a rectangular unit cell ($a = 4.9$ Å, $b = 9.1$ Å, $A_m = 22$ Å^2; see Table 2) containing two molecules related by *b*-glide symmetry in a racemic 2D crystallite.

This monomer proved to be reactive and the best polymerization results were obtained by spreading the monomer on pure water at 4 °C when dimers and trimers were formed after 2.5 h.

The addition of a catalyst ($AgNO_3$ or $CuCl_2$) did not give any longer oligopeptides. However, there was a strong peak in the MALDI−TOF MS that corresponds to the disulfide bridge formation between two C_{18}-ATE thio-alcohol molecules after possible monomer hydrolysis.

3.7. Glu-(C_{18})$_2$. The diester L-Glu-(C_{18})$_2$, which represents a different class of esters bearing two hydrocarbon chains, was reported[11] to yield long oligopeptides; therefore, we reinvestigated the polymerization of films of this monomer. This compound was prepared both as a methylsulfonate salt and as a free amine. The GIXD patterns measured from the 2D crystallites self-assembled from the DL- and L-Glu-(C_{18})$_2$ methylsulfonate salt at a mean molecular area of 55 Å^2 are very similar (Figure 11a and b, respectively). The free amine gave a similar GIXD pattern (not shown). They yielded a rectangular subcell ($a = 5.0$ Å, $b = 8.6$ Å) that contained one molecule tilted along the *a*-axis by 25° from the normal to the water surface. An atomic coordinate molecular model containing a pseudo-herringbone arrangement of the hydrocarbon chains was constructed. The 2D packing arrangement obtained by X-ray-structure-factor-constrained least-squares refinement of the model is shown in Figure 12b and c, together with the corresponding measured and calculated Bragg rod intensity profiles (Figure 12a).

We also measured the GIXD patterns from DL-Glu-(C_{18})$_2$ spread on an aqueous solution of $CuCl_2$ (1 mM). No diffraction was observed at a mean molecular area of 55 Å^2, unlike that observed for the water subphase. The film was then compressed to a mean molecular area of 45 Å^2 and gave the GIXD pattern shown in Figure 11c. The calculated subcell is rectangular ($a = 5.0$ Å, $b = 8.3$ Å) and contains alkyl chains tilted along the *b*-axis by an angle of 18° from the normal to the water surface.

Polymerization experiments performed on the water surface under conditions as previously reported[11] yielded only dimers

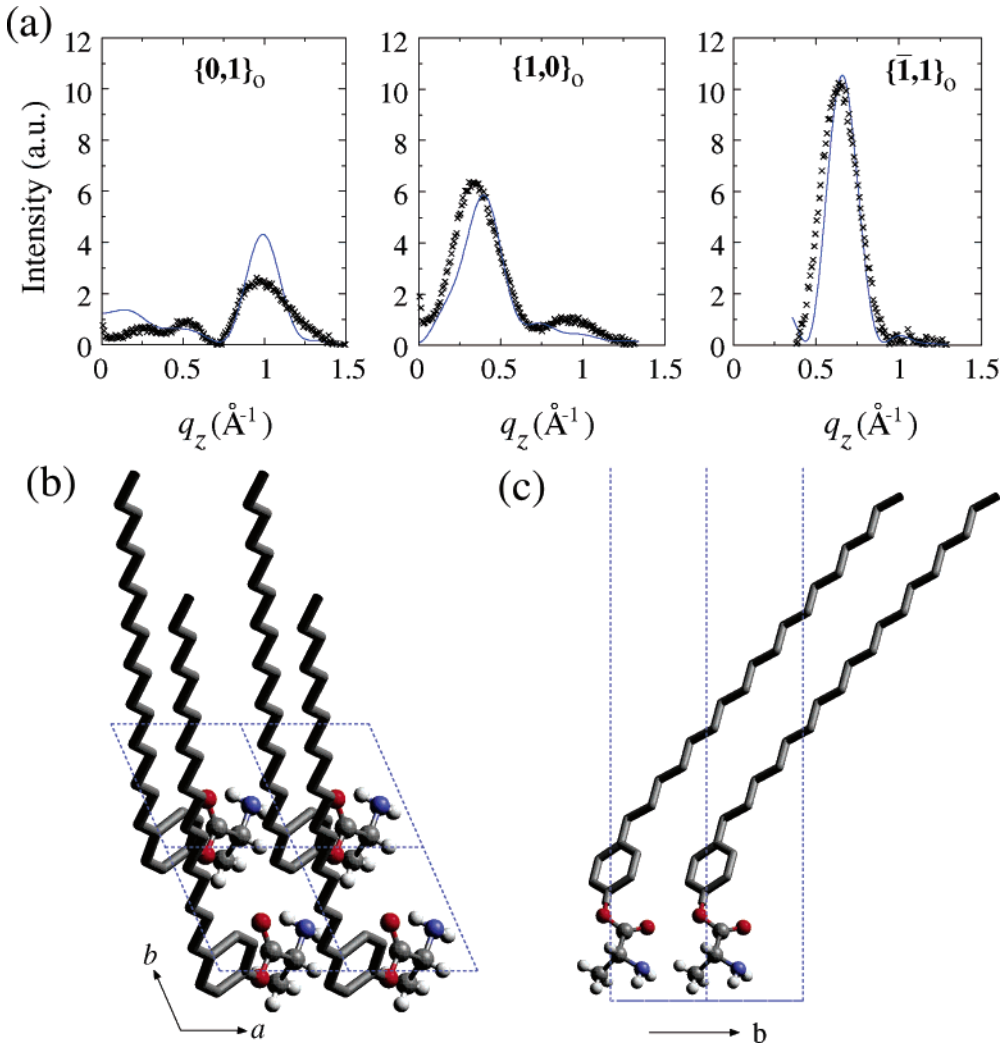

Figure 9. (a) Bragg rod intensity profiles of D-Ala-C_{18}-Ph ((×) measured and (—) calculated). Also shown is the refined packing arrangement of the D-Ala-C_{18}-Ph viewed (b) perpendicular and (c) parallel to the water surface.

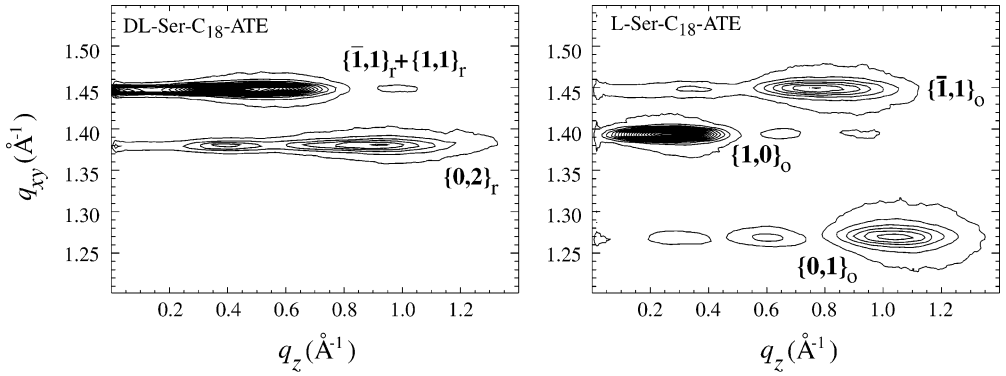

Figure 10. GIXD patterns $I(q_{xy},q_z)$ measured at a mean molecular area of 35 Å^2 from the 2D crystallites self-assembled at the air/water interface from (a) DL-Ser-C_{18}-ATE and (b) L-Ser-C_{18}-ATE. Note that the GIXD patterns of the racemate and the corresponding alcohol (C_{18}-ATE, Figure 4d) are very similar but not identical.

(Scheme 3), as demonstrated by MALDI−TOF MS analysis. The degree of order on the water surface under these conditions (30 °C) is expected to be low. Therefore, we also performed the polymerization on an aqueous subphase at 4 °C, where, again, even in the presence of 1 mM $CuCl_2$ as a catalyst, only dimers were formed.

4. Conclusions

Previous reports have suggested that amphiphilic alkyl esters of α-amino acids self-assemble at the air/solution interface and provide suitable architectures for the generation of peptides by a condensation reactions within a structured environment.[8−11] Here, we report a reinvestigation of some of these reactions by applying grazing incidence X-ray diffractometry (GIXD) and matrix-assisted laser deesorption ionization time-of-flight mass spectroscopy (MALDI−TOF MS) techniques. The packing arrangements of the two-dimensional (2D) crystallites formed by self-assembly at the air/solution interface; both of the amphiphiles reported previously and the new ones were determined by GIXD. The molecular weights were determined

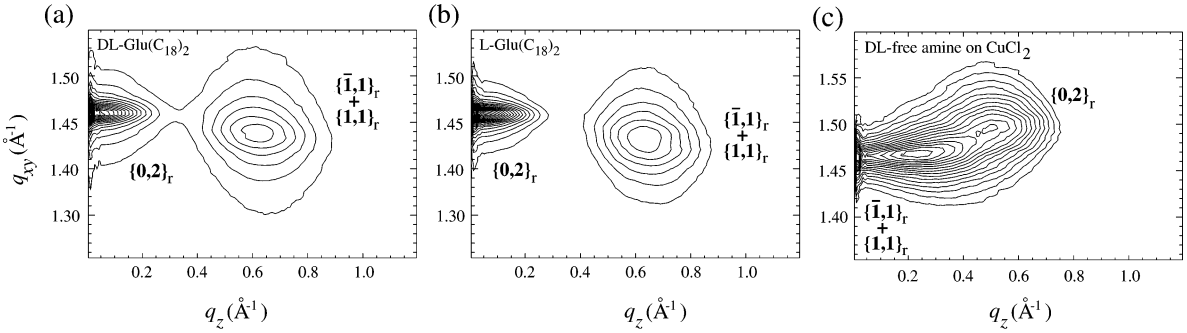

Figure 11. GIXD patterns $I(q_{xy},q_z)$ measured from (a) DL-Glu-$(C_{18})_2$ and (b) L-Glu-$(C_{18})_2$, as methyl sulfonate at a mean molecular area of 55 Å^2, and from (c) DL-Glu-$(C_{18})_2$ free amine at a mean molecular area of 45 Å^2 on 1 mM $CuCl_2$.

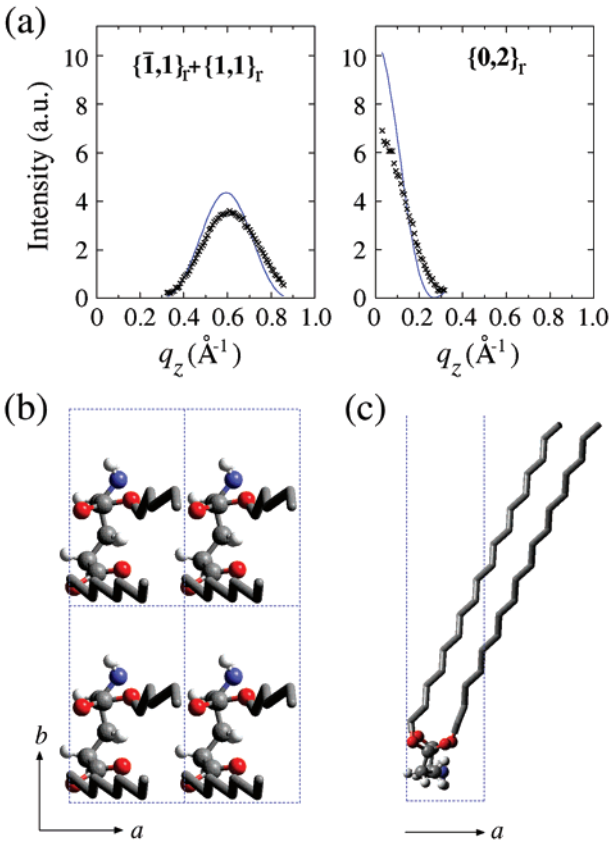

Figure 12. (a) Bragg rod intensity profiles of L-Glu-$(C_{18})_2$ ((×) measured and (—) calculated). Also shown are the refined 2D packing arrangements of L-Glu-$(C_{18})_2$, viewed (b) perpendicular and (c) parallel to the water surface. Note that, for clarity, only portions of the hydrocarbon chains are shown.

SCHEME 3: Dimerization of Glu-$(C_{18})_2$, in Contrast to a Previously Proposed Polycondensation[11]

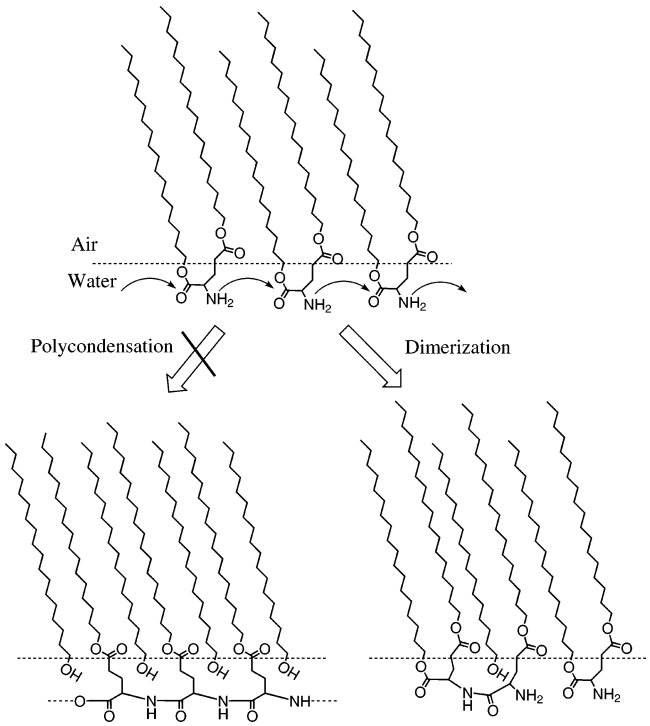

from the MALDI−TOF MS analysis. In all the studied systems, it was found that the polycondensation reaction of the alkyl esters does not proceed beyond the formation of dipeptides.

To generate longer oligopeptides, we investigated also a few alkyl thio-esters, where the alkanethiol is a much better leaving group than the corresponding alkoxy group. In these systems, trimers and tetramers were obtained, in addition to dimers.

To probe the feasibility of generating homochiral oligopeptides by taking advantage of differences in the packing arrangement of racemic versus enantiomorphous 2D crystallites, we have investigated the packing arrangement of several racemic and enantiopure compounds. In the case of Ala-C_{18}-AE, the packing arrangements of L- and DL-crystallites were similar and, in the case of Ala-C_{18}-ATE, almost identical. These results, together with the observation that the distribution of the short oligopeptides formed in the polycondensation of the enantiolabeled racemic monomers is binomial, suggest that the racemate self-assembles in the form of enantiomerically disordered 2D crystallites. It is most plausible that the origin of this disorder is due to the possibility of a methyl group of an Ala moiety of single-handedness to occupy a site of a H atom attached to the stereogenic center of the other enantiomer. It was anticipated that such disorder would not be present in the alkyl esters of α-amino acids such as Phe, Tyr, and Ser, where the side chains are bulkier than those in Ala. However, the esters of racemic and enantiomerically pure Phe and Tyr did not form 2D crystallites at the air/water interface. The Ser esters formed true racemic 2D crystallites; however, they did not react beyond the formation of the corresponding dipeptides and tripeptides.

To rationalize the formation of low-molecular-weight peptides, several possible reasons may be considered. First, these monomers can undergo hydrolysis in addition to polycondensation. The formation of the dipeptides and the alcohol byproduct may induce defects in the crystallites during the early stages of the reaction and change the position of the ester group of the dipeptide—vis a vis, the neighboring amine group—and, thus, hinder further propagation. The product distribution seems to be independent of the coherent length of the various 2D crystallites (Table 2).

Finally, the present results demonstrate that, in contrast to the polycondensation process of amphiphilic thioesters and N^{α}-carboxyanhydride of γ-stearyl-glutamic acid, and N^{ϵ}-stearoyl-lysine,[4,5] systems where, on reaction, longer oligopeptides were formed, the alkyl esters and thio-esters of the amino acids yielded dipeptides and up to tetrapeptides, respectively. Therefore, in contrast to previous reports, they cannot be regarded as useful model systems for the formation of prebiotic peptides, unless more-efficient catalysts for the polycondensation of these esters are discovered.

Acknowledgment. We thank Dr. Gérard Bolbach (Laboratoire de Chimie Structurale Organique et Biologique, Université Pierre et Marie Curie, 75252 Paris Cedex 05, France) for assistance with the MALDI−TOF MS technique development and analysis. We thank the Israel-Science Foundation (ISF) and The Danish Foundation for Natural Sciences for financial support. This work was supported by the IHP (Contract No. HPRI-CT-1999-00040/2001-00140) of the European Community. This work is part of a COST D-27 program. We are grateful to HASYLAB (DESY, Hamburg, Germany) for beam time at the BW1 beamline.

Supporting Information Available: Atomic coordinates of the molecules in the 2D crystallites (PDF). This material is available free of charge via the Internet at http://pubs.acs.org.

References and Notes

(1) Frank, P.; Bonner, W. A.; Zare, R. N. On One Hand But Not the Other: The Challenge of the Origin and Survival of Homochirality in Prebiotic Chemistry. In *Chemistry for the 21st Century*; Keinan, E., Schechter, I., Eds.; Wiley-VCH: Weinheim, 2001; p 175.

(2) Hitz, T.; Luisi, P. L. *Helv. Chim. Acta* **2003**, *86*, 1423.

(3) Weissbuch, I.; Zepik, H.; Bolbach, G.; Shavit, E.; Tang, M.; Jensen, T. R.; Kjaer, K.; Leiserowitz, L.; Lahav, M. *Chem.−Eur. J.* **2003**, *9*, 1782.

(4) Zepik, H.; Shavit, E.; Tang, M.; Jensen, T. R.; Kjaer, K.; Bolbach, G.; Leiserowitz, L.; Weissbuch, I.; Lahav, M. *Science* **2002**, *295*, 1266.

(5) Weissbuch, I.; Bolbach, G.; Zepik, H.; Shavit, E.; Tang, M.; Frey, J.; Jensen, T. R.; Kjaer, K.; Leiserowitz, L.; Lahav, M. *J. Am. Chem. Soc.* **2002**, *124*, 9093.

(6) Weissbuch, I.; Rubinstein, I.; Weygand, M. J.; Kjaer, K.; Leiserowitz, L.; Lahav, M. *Helv. Chim. Acta* **2003**, *86*, 3867.

(7) Rubinstein, I.; Bolbach, G.; Weygand, M. J.; Kjaer, K.; Weissbuch, I.; Lahav, M. *Helv. Chim. Acta* **2003**, *86*, 3851.

(8) Baniel, A.; Frankel, M.; Friedrich, I.; Katchalsky, A. *J. Org. Chem.* **1948**, *13*, 791.

(9) Fukuda, K.; Shibasaki, Y.; Nakahara, H. *J. Macromol. Sci., Chem.* **1981**, *A15*, 999.

(10) Hanabusa, K.; Oumi, T.; Koyama, T.; Shirai, H.; Hayakawa, T.; Kurose, A. *J. Macromol. Sci., Chem.* **1989**, *A26*, 1397.

(11) Fukuda, K.; Shibasaki, Y.; Nakahara, H.; Liu, M. H. *Adv. Colloid Interface Sci.* **2000**, *87*, 113.

(12) Liu, M. H.; Nakahara, H.; Shibasaki, Y.; Fukuda, K. *Chem. Lett.* **1993**, 967.

(13) Liu, M. H.; Nakahara, H.; Shibasaki, Y.; Fukuda, K. *Chem. Lett.* **1994**, 783.

(14) Blout, E. R.; Doty, P.; Yang, J. T. *J. Am. Chem. Soc.* **1957**, *79*, 749.

(15) Blair, N. E.; Bonner, W. A. *Origin Life Evol. Biochem.* **1980**, *10*, 225.

(16) Penney, C. L.; Shah, P.; Landi, S. *J. Org. Chem.* **1985**, *50*, 1457.

(17) Lapidot, Y.; Rappoport, S.; Wolman, Y. *J. Lipid Res.* **1967**, *8*, 142.

(18) Itoh, M.; Hagiwara, D.; Kamiya, T. *Bull. Chem. Soc. Jpn.* **1977**, *50*, 718.

(19) Neises, B.; Steglich, W. *Angew. Chem., Int. Ed. Engl.* **1978**, *17*, 522.

(20) Kuzmenko, I.; Rapaport, H.; Kjaer, K.; Als-Nielsen, J.; Weissbuch, I.; Lahav, M.; Leiserowitz, L. *Chem. Rev.* **2001**, *101*, 1659.

(21) Als-Nielsen, J.; Kjaer, K. In *NATO Advanced Study Institute on Phase Transitions in Soft Condensed Matter* (Geilo, Norway, 1989); Riste, T., Sherrington, D., Eds.; NATO ASI Series, Series B, Physics, Vol. 211; Plenum Press: New York, 1989; p 113.

(22) Kjaer, K. *Physica B* **1994**, *198*, 100.

(23) CERIUS2; Accelrys, Inc: San Diego, CA, 1995.

(24) Sheldrick, G. M. "SHELXL97" Program for the Refinement of Crystal Structures; University of Göttingen, Germany, 1997.

(25) Brunelle, A.; Chaurand, P.; DellaNegra, S.; LeBeyec, Y.; Parilis, E. *Rapid. Commun. Mass Spectrom.* **1997**, *11*, 353.

(26) Majewski, J.; Popovitz−Biro, R.; Bouwman, W. G.; Kjaer, K.; Als-Nielsen, J.; Lahav, M.; Leiserowitz, L. *Chem.−Eur. J.* **1995**, *1*, 304.

(27) Weissbuch, I.; Berfeld, M.; Bouwman, W.; Kjaer, K.; Als-Nielsen, J.; Lahav, M.; Leiserowitz, L. *J. Am. Chem. Soc.* **1997**, *119*, 933.

(28) The GIXD spectra of the D-, L-, and deuterated L-Ala-C18-AE were measured and yielded identical results. DL-Ala-C18-AE was measured both from a 1:1 mixture of the enantiomers and from the racemate synthesized from racemic alanine and yielded identical patterns.